Strong competition between the δl and δT_c flux pinning mechanisms in MgB_2 doped with carbon containing compounds

S. R. Ghorbani,[1,2] Xiao-Lin Wang,[1,a)] M. S. A. Hossain,[1] Q. W. Yao,[1] S. X. Dou,[1] Sung-IK Lee,[3,b)] K. C. Chung,[4] and Y. K. Kim[4]
[1]*Institute for Superconducting and Electronic Materials, University of Wollongong, Wollongong, New South Wales 2522, Australia*
[2]*Department of Physics, Sabzevar Tarbiat Moallem University, P.O. Box 397, Sabzevar, Iran*
[3]*National Creative Research Initiative Center for Superconductivity, Department of Physics, Sogang University, Seoul 121-742, Republic of Korea*
[4]*Nano-functional Materials Group, Korea Institute of Materials Science, Changwon, Republic of Korea*

(Received 5 August 2009; accepted 18 February 2010; published online 10 June 2010)

The transport and magnetic properties of 10 wt % malic acid and 5 wt % nanocarbon doped MgB_2 have been studied by measuring the resistivity (ρ), critical current density (j_c), connectivity factor (A_F), irreversibility field (H_{irr}), and upper critical field (H_{c2}). The pinning mechanisms are studied in terms of the collective pinning model. It was found that both mean free path (δl) and critical temperature (δT_c) pinning mechanisms coexist in both doped MgB_2. For both the malic acid and nanocarbon doped samples, the temperature dependence of the crossover field, which separates the single vortex and the small bundle pinning regime, $B_{sb}(T)$, shows that the δl pinning mechanism is dominant for temperatures up to $t(T/T_c)=0.7$ but the δT_c pinning mechanism is dominant for $t>0.7$. This tendency of coexistence of the δl and the δT_c pinning mechanism is in strong contrast with the pure MgB_2, in which the δT_c pinning mechanism is dominant over a wide temperature range below T_c. It was also observed that the connectivity factor, active cross-sectional area fraction (A_F), are 0.11 and 0.14 for the nanocarbon and the malic acid doped MgB_2, respectively, indicating that there are still rooms for further improving j_c performance. © *2010 American Institute of Physics*. [doi:10.1063/1.3366710]

I. INTRODUCTION

Enhancement of the critical current density has been a central topic of research since the discovery of superconductivity in magnesium diboride (MgB_2), where the critical temperature (T_c) ≈ 39 K.[1] High critical current density values of 10^5-10^6 A/cm^2 have been reported for this superconductor. However, the critical current density (j_c) drops rapidly with increasing temperature and magnetic field. The j_c is controlled by many parameters, e.g., the irreversibility field (H_{irr}), the upper critical field (H_{c2}), the flux pinning, and the connectivity. There are two ways to improve j_c. The first one is the improvement of the intrinsic properties, such as the irreversibility field H_{irr} and the upper critical field H_{c2}. The second involves increasing j_c through improvement of extrinsic properties, such as by decreasing porosity and increasing connectivity. The research toward improvement of j_c properties in MgB_2 has been mostly aimed at enhancing the H_{irr}, the flux pinning ability, and H_{c2} by irradiation or chemical doping.[2–8] Chemical doping has been proved to be a simple and effective way to introduce pinning centers into MgB_2 superconductor or to improve the upper critical field. It is believed that carbon containing dopants, such as nano-SiC,[5] carbon nanotubes,[6] nanocarbon,[7] hydrocarbons,[8] silicone oil,[9,10] malic acid,[11] etc., are especially effective in enhancing the H_{c2}, and hence the j_c properties of MgB_2 in high magnetic fields.

Intergrain boundary pinning[12] and point defect pinning[13] are the two main important pinning mechanisms used to improve j_c. In high-κ type-II superconductors, where κ is the Ginzburg–Landau parameter, the most important elementary interaction between the vortices and the pinning centers is the core interaction. It arises from the influence of the parts of the material with weak superconducting properties on the spatial variation in the superconducting order parameter. The core interaction that is generally prevalent is magnetic in nature and related to the presence of interfaces parallel to the external field between superconducting and nonsuperconducting regions. It has been found that in MgB_2 bulk and thin film samples, with κ larger than 20,[14,15] the core pinning is related to randomly distributed spatial variations in the transition temperature (δT_c pinning).[16,17] However, in the high-temperature superconductors, the core interaction is associated with charge-carrier mean free path variations (δl pinning), mostly due to crystal lattice defects.[18]

The critical current density of MgB_2 has been improved by more than one order of magnitude, especially in high magnetic field by adding SiC.[5] It has also been found that maximum flux pinning forces are increased by decreasing grain size.[19] Therefore, the size of the doping is particularly important in doped MgB_2 samples. It is effective to reduce the grain size of MgB_2 by chemical doping approach, such as nano-SiC, nano-C, or nano-Si, or using liquid precursors,

a)Electronic mail: xiaolin@uow.edu.au.
b)Prof. Sung-Ik Lee, one of our original corresponding authors, sadly passed away in February 2010 before this paper could be published.

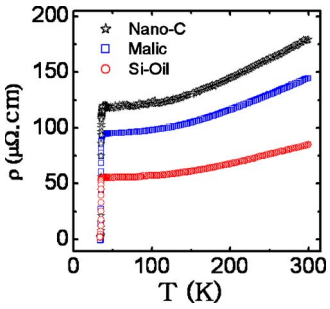

FIG. 1. (Color online) The electrical resistivity ρ vs temperature T for the 10 wt % malic acid doped and the 5 wt % nanocarbon doped sample sintered at 800 °C. For comparison, data from Ref. 10 for the 10 wt % silicone oil doped sample sintered at 600 °C are also shown.

such as silicone oil and other oxide or nonoxide nanomaterials.[5–11,19,20] Improvement of the $j_c(B)$ was quite successful for most of chemical doped MgB_2. However, the origin of the pinning mechanisms are still not well understood except the silicon oil doped case.[10]

In this paper, the effects of two kinds of carbon sources, in the form of nanocarbon and malic acid doped MgB_2 samples were studied. The origin of the improvement of $j_c(B)$ and vortex pinning mechanism for above cases are analyzed in the framework of the collective pinning theory and compared with the silicon oil doped case. Compare to the δT_c pinning for the pure MgB_2 over the whole temperature range below T_c, both δl and δT_c pinning coexist in the MgB_2 doped with above two kinds of carbon sources.

II. EXPERIMENTAL

The standard solid state powder processing technique was adapted to prepare the 10 wt % malic acid and 5 wt % nano-C added polycrystalline MgB_2 samples after the sintering at temperature of 800 °C as described elsewhere.[21] The critical temperature T_c was defined as the onset temperature at which diamagnetic properties were observed. This temperature was 35 ± 0.20 K for the both samples. X-ray diffraction results revealed that all samples were crystallized in the MgB_2 structure as the major phase. However, a few impurity lines of MgO in the both samples were observed. The resistivity measurements were carried out on the bare cylindrical bar samples by using a physical properties measurement system (PPMS, Quantum Design) in the field range from 0–8.7 T. The magnetic hysteresis loops were measured using a magnetic property measurement system (MPMS, Quantum Design). By using the Bean's critical state model, the critical current density was calculated.

III. RESULTS AND DISCUSSIONS

The temperature dependencies of the resistivity (ρ) for the MgB_2 samples with different dopants at zero external magnetic fields are shown in Fig. 1. For comparison, data from Ref. 10 for silicone oil doped MgB_2 with similar T_c are also shown. It can be seen that the resistivity depends on the particular dopant. Table I presents the measured ρ values, the residual resistivity ratio, RRR ($\rho_{300\ K}/\rho_{40\ K}$), and the active cross-sectional area fraction (A_F) of MgB_2 samples for three

TABLE I. The resistivity at 40 and 300 K, $\Delta\rho=\rho_{300\ K}-\rho_{40\ K}$ and the connectivity factor A_F of 5 wt % nanocarbon, 10 wt % malic acid, and 10 wt % silicone oil doped MgB_2. The resistivity data for the silicone oil doped MgB_2 sample are extracted from Ref. 10.

Sample	$\rho_{40\ K}$ ($\mu\Omega$ cm)	$\rho_{300\ K}$ ($\mu\Omega$ cm)	$\Delta\rho$ ($\mu\Omega$ cm)	A_F
Nanocarbon	119.4	180.4	61.0	0.111
Malic acid	94.9	145.2	50.3	0.145
Silicone oil	55.5	85.3	29.8	0.249

different dopants. The results show that ρ in the normal state for silicone oil doped MgB_2 is lower than for the nanocarbon and malic acid doped superconductors. Therefore, the scattering processes are different in these samples.

The connectivity factor, A_F, from the relation $A_F=\Delta\rho_{sc}/\Delta\rho$, where $\Delta\rho_{sc}$ is the single crystal resistivity and $\Delta\rho=\rho(300\ K)-\rho(40\ K)$, from our experimentally measured resistivity, was also evaluated by the Rowell analysis.[22] We observed that A_F of the silicone oil doped sample was larger than that of the malic acid doped sample, as well as the nanocarbon doped sample. As can be seen in Table I, A_F values ranged from as low as 0.111 (nano-C doped MgB_2) to as high as 0.249 (Si-doped MgB_2), depending on the dopant. However, the A_F values of all samples are still lower than the ideal value of 1. This indicates that there are some obstacles to current, such as voids or the impurities MgO for all samples.

The $j_c(B,T)$ results are shown in a double-logarithmic plot in Fig. 2 at the temperatures of 20 and 30 K for all samples. The published data for the silicone oil doped MgB_2 (Ref. 10) is added in Fig. 2. The $j_c(B,T)$ values for the nanocarbon and malic acid doped MgB_2 are almost same, while the silicone oil doped MgB_2 has a larger j_c. For all the samples, the j_c initially shows a plateau at low field and then begins to decrease quickly once the field reaches the crossover field from the single vortex to the small bundle pinning regime, B_{sb}, which decreases with increasing temperature. Further increasing the field results in a faster drop in j_c near the irreversibility line, which is obtained by using the criterion of $j_c=100\ A/cm^2$.

The normalized temperature dependence of B_{c2}, which was obtained from the 90% values of their corresponding resistivity transitions and of B_{irr} are shown in Fig. 3. The results show that B_{c2} depends on the dopant while B_{irr} does

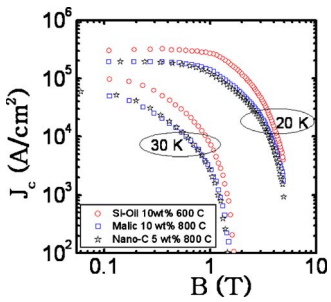

FIG. 2. (Color online) Magnetic dependence of the critical current density j_c for malic acid and nanocarbon doped MgB_2. Results for j_c of silicone oil doped MgB_2 (Ref. 10) are also shown.

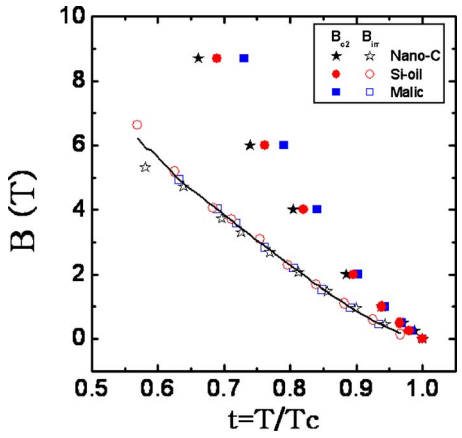

FIG. 3. (Color online) The upper critical and irreversibility fields of 10 wt % malic acid, 5 wt % nanocarbon, and 10 wt % silicone oil doped MgB_2 as a function of temperature. The solid curves are fits to $B_{irr}=B_{irr}(0)[1-(T/T_c)^2]^{3/2}$, with fitting parameter $B_{irr}(0)$. Data for silicone oil doped MgB_2 sample have been taken from Ref. 10.

not. The solid curves in Fig. 3 are in good agreement with the typical behavior expected for the case of giant flux creep, which is predicted to be $B_{irr}\approx(1-t^2)^{3/2}$, where $t=T/T_c$.[23]

The collective pinning theory which was derived by Blatter *et al.*,[23] shows that critical current density is field independent if the applied magnetic field is lower than the crossover field B_{sb}. In this low field limit, the interaction between the vortices is negligible and a single vortex pinning mechanism dominates with following relation:

$$B_{sb}\propto j_{sv}B_{c2}, \tag{1}$$

where j_{sv} is the critical current density. At higher fields, for $B>B_{sb}$, $j_c(B)$ decreases quickly as field is increased and critical current density follows an exponential form:

$$j_c(B)\approx j_c(0)\exp[-(B/B_0)^{3/2}], \tag{2}$$

where B_0 is a parameter of the order of B_{sb}.

Whether experimental results $j_c(B)$ as shown in Fig. 2 follows the Eq. (2) or not, $-\log[j_c(B)/j_c(0)]$ as a function of B is drawn in a double-logarithmic plot in the inset of Fig. 4. It is clear that Eq. (2) describes the experimental data quite well for intermediate fields, while deviations from the fitting curves are observed at both low and high fields. The deviation at low fields, below B_{sb}, is from the single vortex pinning regime to the small bundle pinning regime. The deviation at high field is located near to the irreversibility line, which is related to thermal fluctuation effect. The field of this deviation is indicated as B_{th}.

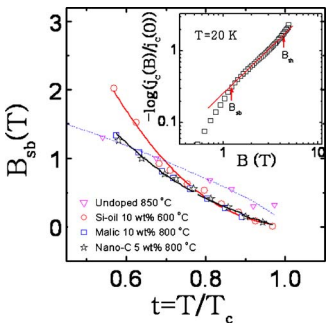

FIG. 4. (Color online) Normalized temperature dependence of the crossover field B_{sb}. The solid curves are fits to Eq. (4). Inset: double logarithmic plot of $-\log[j_c(B)/j_c(0)]$ as a function of B, with the solid line showing the fit given by Eq. (2). The crossover fields B_{sb} and B_{th} are shown by arrows. The data for the silicone-oil doped and undoped samples are extracted from Refs. 10 and 24, respectively.

The crossover field B_{sb} while varying temperature is drawn in Fig. 4 for pristine MgB_2 sintered at 850 °C, the 10 wt % malic acid doped, and the 5 wt % nanocarbon doped samples. For the comparison, we added data of 10 wt % silicone oil doped, from ours previous publication.[10] The results show that the silicone oil (liquid precursor) doped MgB_2 has a larger B_{sb} value than that of the malic acid and the nanocarbon doped MgB_2. These results shows that the liquid precursor, silicone oil, which produces Si and C on the atomic scale, enhance the connectivity and further improve the j_c and the crossover field B_{sb} of MgB_2.

It is known that the δT_c and δl pinning show different temperature dependencies of the critical current density j_{sv} in the single vortex pinning regime as $j_{sv}\propto(1-t^2)^{7/6}(1+t^2)^{5/6}$, with $t=T/T_c$ and for the case of δT_c pinning, while for δl pinning, $j_{sv}\propto(1-t^2)^{5/2}(1+t^2)^{-1/2}$.[17,18] Unified version of B_{sb} is as following:

$$B_{sb}(T)=B_{sb}(0)\left(\frac{1-t^2}{1+t^2}\right)^{\upsilon}, \tag{3}$$

where $\upsilon=2/3$ and 2 for δT_c and δl pinning, respectively.

To find out how much of the δT_c and δl pinning contribute the total pinning mechanism of the doped MgB_2 samples, we separated the B_{sb} data into two part as follows:

$$B_{sb}=P_1B_{sb}^{T_c}+P_2B_{sb}^{l}, \tag{4}$$

in which $B_{sb}^{T_c}$ and B_{sb}^{l} are the B_{sb} for of δT_c and δl pinning, respectively. The values of P_1 and P_2 are fitting parameters of δT_c and δl pinning. In order to compare the effects of the δT_c and the δl pinning mechanisms, the P parameter was defined $P_{T_c}=P_1B_{sb}^{T_c}/B_{sb}$ and $P_l=P_2B_{sb}^{l}/B_{sb}$, which represent δT_c or δl pinning effects, respectively. The B_{sb} data obtained from inset of Fig. 4 follows Eq. (4) very well as shown in the solid curves in Fig. 4.

From Fig. 4, one can immediately notice that the B_{sb} of pure MgB_2 is quite different from those of the above three types of nanoparticles doped MgB_2. The contributions of each pinning effect are shown in Fig. 5. For both doped MgB_2, both δT_c pinning and δl pinning exist but which pinning mechanism is dominant depends on the temperature range and dopants. In particular, δl pinning is the dominant mechanism at low temperatures but with increasing temperature δT_c pinning becomes dominant. From Fig. 5, one can clearly see the change from the δl to δT_c pinning mechanism at $t\approx0.7$. The contributions of each pinning for the malic acid and nano-C doped MgB_2 are compared with the silicone oil doped MgB_2 (data extracted from the Ref. 10) and the undoped MgB_2 from the Ref. 24, as shown in the Fig. 6. The results clearly shows that the δT_c pinning is dominant over the whole temperature range for the pristine MgB_2.[16] For three doped MgB_2 samples, the dominating pinning mechanism depends on the temperature range and dopants. The temperature T_{eq} where both pinning mechanisms have equal contributions depends on the dopant as well. The T_{eq} values

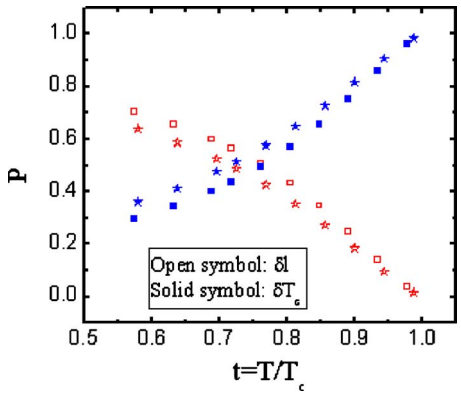

FIG. 5. (Color online) δl and δT_c pinning contributions as a function of normalized temperature for 10 wt % malic acid doped (squares) and 5 wt % nanocarbon doped MgB_2 sintered at 800 °C (stars).

are 32.5, 26.5, and 24.6 K for silicone oil,[10] malic acid, and nanocarbon doped MgB_2 samples, respectively. These results suggest that the δl is the dominant for both nanocarbon and malic acid doped MgB_2 for $t \approx 0.7$, while for the silicone oil doped sample this pinning is dominant upto the temperatures close to the T_c.

In conclusion, we have found that MgB_2 doped with a liquid precursor, silicone oil,[10] in MgB_2 results show higher grain connectivity and larger $j_c(B)$ compared to nonliquid carbon sources of malic acid and nano-C doped MgB_2 even though this nonliquid carbon sources gave high improvement of $j_c(B)$ compare to the pristine MgB_2. Our results show that the δl pinning mechanism, due to spatial fluctuations of the charge-carrier mean free path, is dominant at low temperatures in MgB_2 doped with malic acid, nanocarbon, and silicone oil,[10] while at high temperatures close to T_c, δT_c pinning is the dominant pinning mechanism. We found that the increase in the critical current density for the malic acid and nano-C doped MgB_2 is very much related to the change of the doping mechanism from δT_c to δl pinning and the increase in $B_{sb}(T)$.

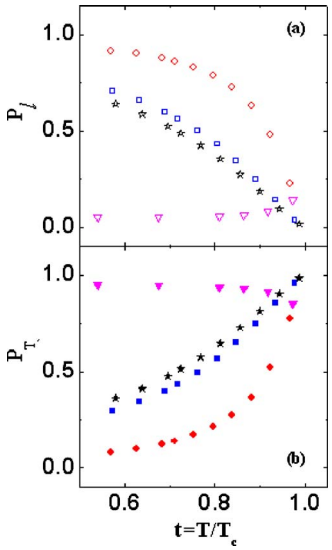

FIG. 6. (Color online) (a) δl pinning and (b) δT_c pinning contributions as a function of normalized temperature for undoped MgB_2 sintered at 850 °C (triangles), 10 wt % malic acid doped (squares), 5 wt % nanocarbon doped MgB_2 sintered at 800 °C (stars), and 10 wt % silicone oil doped MgB_2 sintered at 600 °C (circles) from Ref. 10.

ACKNOWLEDGMENTS

This work is supported by the Australian Research Council. It was also supported by the Global Partnership Program from the National Research Foundation through a grant provided by the Korean Ministry of Education, Science and Technology (Grant No. M60602000012).

[1] G. J. Nagamatsu, N. Nakagawa, T. Muranaka, Y. Zenitali, and J. Akimitsu, Nature (London) **410**, 63 (2001).
[2] Y. Bugoslavsky, L. F. Cohen, G. K. Perkins, M. Polichetti, T. J. Tate, R. Gwilliam, and A. D. Caplin, Nature (London) **411**, 561 (2001).
[3] X. Z. Liao, A. C. Serquis, Y. T. Zhu, J. Y. Huang, D. E. Peterson, F. M. Mueller, and H. F. Xu, Appl. Phys. Lett. **80**, 4398 (2002).
[4] M. Eisterer, M. Zehetmayer, S. Tonies, H. W. Weber, M. Kambara, N. H. Babu, D. A. Cardwell, and L. R. Greenwood, Supercond. Sci. Technol. **15**, L9 (2002).
[5] S. X. Dou, S. Soltanian, J. Horvat, X. L. Wang, S. H. Zhou, M. Ionescu, H. K. Liu, P. Munroe, and M. Tomsic, Appl. Phys. Lett. **81**, 3419 (2002).
[6] S. X. Dou, W. K. Yeoh, J. Horvat, and M. Ionescu, Appl. Phys. Lett. **83**, 4996 (2003).
[7] Y. W. Ma, X. P. Zhang, G. Nishijima, K. Watanabe, S. Awaji, and X. D. Bai, Appl. Phys. Lett. **88**, 072502 (2006).
[8] H. Yamada, M. Hirakawa, H. Kumakura, and H. Kitaguchi, Supercond. Sci. Technol. **19**, 175 (2006).
[9] X. L. Wang, Z. X. Cheng, and S. X. Dou, Appl. Phys. Lett. **90**, 042501 (2007).
[10] S. R. Ghorbani, X. L. Wang, S. X. Dou, S.-IK Lee, and M. S. A. Hossain, Phys. Rev. B **78**, 184502 (2008).
[11] M. S. A. Hossain, J. H. Kim, X. Xu, X. L. Wang, M. Rindfleisch, M. Tomic, M. D. Sumption, E. W. Collings, and S. X. Dou, Supercond. Sci. Technol. **20**, L51 (2007).
[12] S. Lee, H. Mori, T. Masui, Y. Eltsev, A. Yamamoto, and S. Tajima, J. Phys. Soc. Jpn. **70**, 2255 (2001).
[13] S. X. Dou, X. L. Wang, J. Horvat, D. Milliken, E. W. Collings, and M. D. Sumption, Physica C **361**, 79 (2001).
[14] C. Buzea and T. Yamashita, Supercond. Sci. Technol. **14**, R115 (2001).
[15] D. K. Finnemore, J. E. Ostenson, S. L. Bud'ko, G. Lapertot, and P. C. Canfield, Phys. Rev. Lett. **86**, 2420 (2001).
[16] M. J. Qin, X. L. Wang, H. K. Liu, and S. X. Dou, Phys. Rev. B **65**, 132508 (2002).
[17] S. L. Prischepa, M. L. Della Rocca, L. Maritato, M. Salvato, R. Di Capua, G. Maglione, and R. Vaglio, Phys. Rev. B **67**, 024512 (2003).
[18] R. Griessen, W. Hai-hu, A. J. J. van Dalen, B. Dam, J. Rector, and H. G. Schnack, Phys. Rev. Lett. **72**, 1910 (1994).
[19] E. Martínez, P. Mikheenko, M. Martínez-López, A. Millán, A. Bevan, and J. S. Abell, Phys. Rev. B **75**, 134515 (2007).
[20] J. Karpinski, N. D. Zhigadlo, G. Schuck, S. M. Kazakov, B. Batlogg, K. Rogacki, R. Puzniak, J. Jun, E. Müller, P. Wägli, R. Gonnelli, D. Daghero, G. A. Ummarino, and V. A. Stepanov, Phys. Rev. B **71**, 174506 (2005).
[21] J. H. Kim, S. X. Dou, M. S. A. Hossain, X. Xu, J. L. Wang, D. Q. Shi, T. Nakane, and H. Kumakura, Supercond. Sci. Technol. **20**, 715 (2007).
[22] J. M. Rowell, Supercond. Sci. Technol. **16**, R17 (2003).
[23] G. Blatter, M. V. Feigel'man, V. B. Geshkenbein, A. I. Larkin, and V. M. Vinokur, Rev. Mod. Phys. **66**, 1125 (1994).
[24] J. L. Wang, R. Zeng, J. H. Kim, L. Lu, and S. X. Dou, Phys. Rev. B **77**, 174501 (2008).